

**Seismic anisotropy beneath the northeastern United States: An investigation  
of SKS splitting at long-running seismic stations**

Ivette López

*Adviser: Maureen Long  
Second Reader: Jeffrey Park*

May 4, 2016

A Senior Essay presented to the faculty of the Department of Geology and Geophysics,  
Yale University, in partial fulfillment of the Bachelor's Degree.

In presenting this essay in partial fulfillment of the Bachelor's Degree from the Department of Geology and Geophysics, Yale University, I agree that the department may make copies or post it on the departmental website so that others may better understand the undergraduate research of the department. I further agree that extensive copying of this thesis is allowable only for scholarly purposes. It is understood, however, that any copying or publication of this thesis for commercial purposes or financial gain is not allowed without my written consent.

Ivette López, 04 May 2016

## Abstract

Throughout geologic time, there have been numerous deformation events in Earth's history. Seismic anisotropy allows for the observation of seismic waves as they travel through the upper mantle and crust. More specifically, shear wave splitting patterns in an anisotropic medium distinguish between heterogeneous and homogeneous material in Earth's interior. For example, the alignment of minerals such as olivine affect wave propagation in the mantle; therefore, measurements of anisotropy provide constraints on mantle convection and flow. The ultimate goal is to establish a connection among SKS splitting parameters, local geology, and deformation in the northeastern United States. When measuring anisotropy beneath New England, it has been observed that both the lithosphere and asthenosphere contribute to the complex record of past and present deformational processes in the mantle. Previous studies have also determined variable anisotropy across the eastern United States, citing the Appalachian mountain chain as a source of lithospheric deformation. The increasing availability of seismic data at long-running seismic stations allows for a more comprehensive view, which further constrains deformation in Earth's mantle. Therefore in this study, I analyze seven stations across the northeastern United States with improved time coverage spanning 10+ years expanding on previous observations. I obtain results with extensive backazimuthal coverage, ensuring an accurate representation of shear wave splitting. I detect evidence for multiple layers of anisotropy, which contributes to the apparent isotropy at one of the stations (HNN) characterized by only null results. The surrounding stations demonstrate SKS splitting consistent with results from earlier studies, but with additional detail. However, complex anisotropy limits our ability to distinguish signals from the lithosphere and asthenosphere, thus complicating our understanding of deformation processes. Current models will need to be adjusted to address variations in geometry of deformation as well as mantle flow processes. Overall, my results provide insight on the dynamic processes occurring in Earth's interior suggesting complex anisotropy, with signatures from the uppermost layers. This is consistent with previous data that also illustrate small scale variations in the mantle. We must also recognize this information in the larger context of global tectonics, such as continental collisions, orogeny, and rifting. As additional techniques are developed and arrays are placed, limitations in seismic anisotropy will diminish. This study contributes to our current understanding of past and present-day deformation processes, the extent of Appalachian influence on local surface geology, and the relationship between seismic anisotropy and mantle flow.

## I. Introduction

Seismic anisotropy describes the variation of seismic wave velocities as a result of polarization and propagation direction. In addition, anisotropy reveals information on the deformation in the both the upper crust and mantle (Long and Silver, 2009). More specifically, mantle rocks that contain minerals such as olivine have anisotropic properties. The lattice preferred orientation (LPO) of mineral grains reveals deformation and flow in the mantle (Long *et al.*, 2015). Rock fabric and structural features such as cracks, pores, sheets, and crystal lattices may cause seismic anisotropy or varying wave speeds. A material's elastic properties may also affect anisotropy (Long and Silver, 2009). The particle interactions inside a solid or a liquid will determine the energy and velocity that is transferred through the medium. Therefore, seismic anisotropy provides crucial information about the geological processes and mineralogy inside Earth.

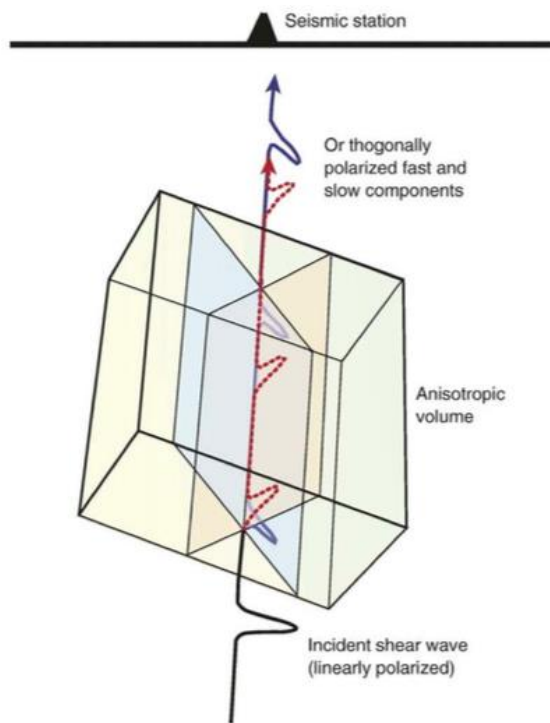


**Fig. 1:** Schematic diagram of a shear wave splitting into two constituents when passing through an anisotropic medium. (From Long and Becker, 2010)

When a shear wave enters an anisotropic medium, it splits into two polarized components (Figure 1). Each polarized shear wave propagates at a different velocity, such as slow and fast, with orthogonal directions as well. The first shear wave (blue) will have a higher velocity and will be parallel to the fractures and fast direction of a medium (Long and Becker, 2010). The splitting parameter  $\varphi$  represents the polarization direction of the fast component. However, the second wave will propagate much slower with an orthogonal orientation. Since the fast and slow components are traveling at different velocities, they will accumulate a time delay parameter of  $\delta t$  (Long and Becker, 2010). The polarization of shear waves and these parameters provide insight on the internal structure, specifically the strength and geometry of the medium it passes through. Shear wave splitting data has been used to observe mantle flow direction, deformation in the lithosphere and crust, and thickness of various layers

(Long and Silver, 2009). However, anisotropy below continental plates is complex because it can be attributed to wide range of processes such as the present local plate motion or past tectonic events resulting in various uncertainties. Therefore a comprehensive survey is necessary to successfully distinguish past and present deformation processes as well as the contributing layers.

In this study, I examined seismic data from various localities in the northeastern United States. These seismic stations have been running for a long period time; therefore, display consistent information on the complexity of seismic anisotropy by constraining it within the asthenosphere and lithosphere. In addition, the seismic stations provide an extensive geographic range across six different states (CT, ME, MA, NH, NY, and PA) as well as temporal coverage of the northeastern United States (Figure 2). I conducted shear wave splitting measurements at seven seismic stations for events greater than 5.7 M in the northeastern United States and reviewed ~500 seismograms for most stations. Stations were chosen based on two factors, running time and distance between one another, with the goal of examining stations over a large region.

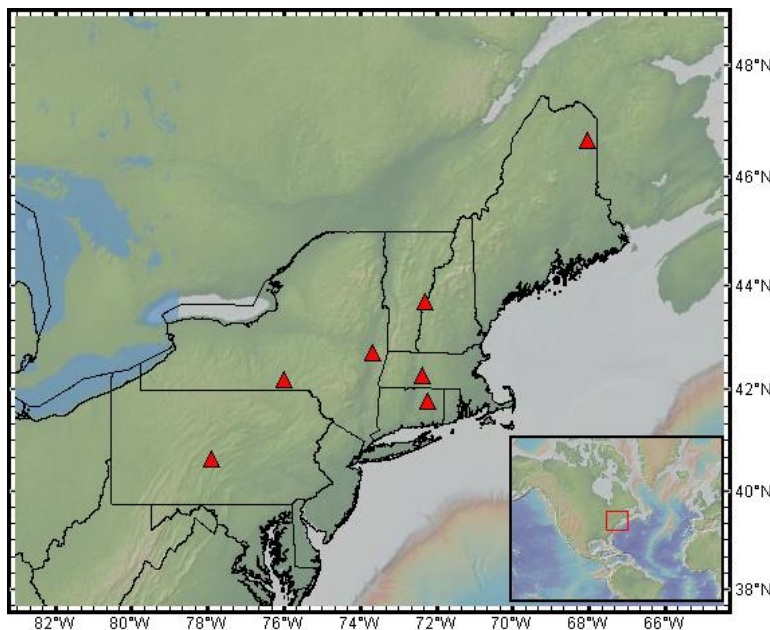


**Fig. 2:** This map displays northeastern U.S. state boundaries with seismic station locations that were analyzed. (Created using GeoMap Application)

I interpret these results as reflecting multiple layers of anisotropy. For example, at several stations (BINY, PQI, QUA2, and SSPA) there are instances of weak splitting, which signal to complex anisotropy. In addition, station HNH (Hanover, NH) does not show evidence of SKS splitting, but instead provides null results over an extensive range of backazimuths, which further supports the idea of multiple layers. Unfortunately, the TRY (Troy, NY) and UCCT (Mansfield, CT) stations provided limited data on anisotropy due to unforeseen problems with the seismometers. Overall, this long-running data is consistent with the presence of multiple layers of anisotropy over a large backazimuthal variation.

## II. Study Area: The Appalachians

Here I present a brief overview of the Appalachian orogeny, closely based on the Hatcher (2010) summary. Today the Appalachian Mountains extend across the eastern U.S. from northern Newfoundland to the Coastal Plain of Alabama and Georgia where the mountains are less exposed and lie beneath the surface (Hatcher, 2010). There is varying deformation across the orogen, for example near New York City, the Appalachians transition into a narrower mountain belt, but north and south of this area the belt widens (Hatcher, 2010). The geological map below displays the distribution of rocks and formations across the northeastern United States (Figure 3). Heterogeneity in geologic strata may help explain the origin of complex anisotropy observations.

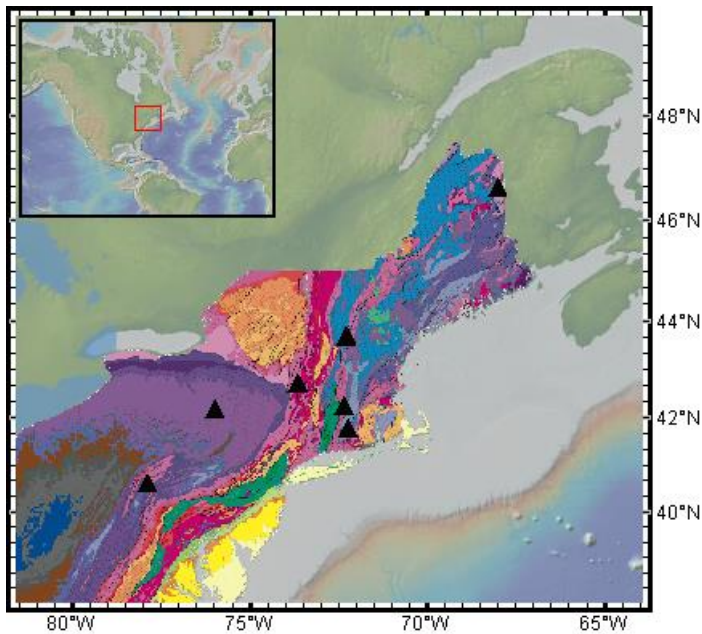


**Fig. 3:** Geologic characteristics of northeastern United States represented by various colors and stations superimposed in black. (Created with GeoMapp Application)

At around 1 Ga, supercontinent Rodinia assembled and was associated with the mountain building event: the Grenville orogeny (Hatcher, 2010). When supercontinent Rodinia separated (~750 Ma), the Appalachian orogen formed during a series of continental collisions, rifting, and orogenesis. This marked the end of the Middle Proterozoic Wilson cycle, where continental rifting created the irregular Laurentian margin and opened the Iapetus Ocean. Eventually, the Paleozoic Era (~540-250 Ma), concluded with the formation of Pangaea and the completion of the Appalachian Wilson cycle in eastern Laurentia, which created the accretionary orogen (Hatcher, 2010).

Although a platform margin and peri-Gondwanan elements are observed throughout the Appalachians, deformation and accretion occurred at different rates across this mountain range (Hatcher, 2010). For example, the Appalachians are comprised of three diachronous events: the Ordovician-Taconic orogeny, Acadian-Neoacadian orogeny, and the Alleghanian orogeny (Figure 4 below).

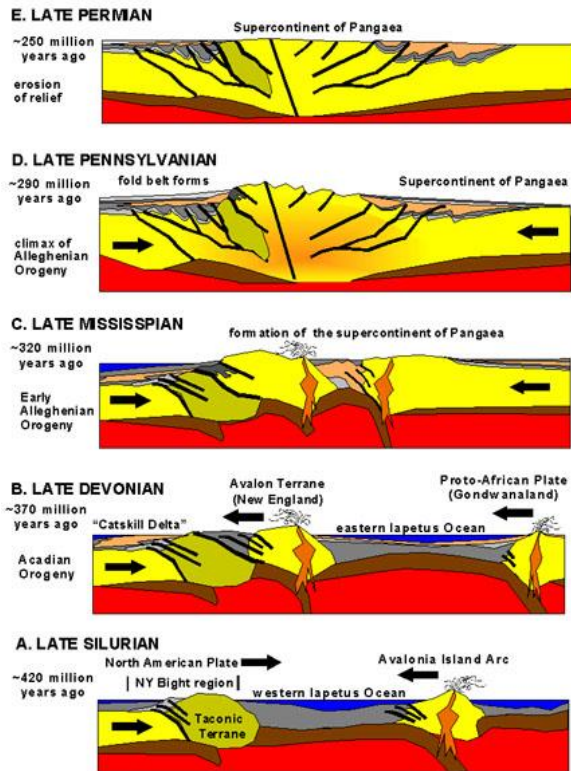


**Fig. 4:** Diagram illustrating continental collisions involved in the formation of the Appalachians during three major orogenic events. (Courtesy of the USGS)

The Ordovician Taconic orogeny (~450-435 Ma) occurred when the Iapetus oceanic plate subducted below the North American craton, which led to volcanism and uplift along the continental margin. This was followed by the Acadian-Neoacadian orogeny (~375-325 Ma), which involved oblique convergence between the Laurasian continent and Avalonian terranes along a strike-slip fault. Finally, the Alleghenian orogeny (~325-260 Ma) consisted of continental collisions between the Euramerica and the African supercontinent, where the greatest deformation

occurred in the Southern Appalachians, but extends northeast as well. In addition, Hatcher (2010) attributes the Silurian-Salinic orogeny to the Northern and Central Appalachians. These past deformation events contribute to the present complex structure and geometry of Earth's interior, specifically the signals from the upper mantle.

### III. Previous anisotropic studies in the eastern U.S.

Previous studies provide an excellent motivation for this the work I present here, which provides further testing and analysis of past studies' results contributing to the ongoing discussion of complex anisotropy by conducting SKS analyses on long-running seismic stations.

Several studies have investigated anisotropy along the eastern United States, specifically the Appalachians. Barruol *et al.*, (1997) performed one of the earliest anisotropy studies in the eastern U.S. They sampled 120 seismic events from 23 long-period stations (~18 mos.), including BINY and SSPA, for SKS, SKKS, and PKS arrivals as well as splitting parameters:  $\Delta t$  and  $\theta$ . They obtained 600 splitting measurements and concluded a strong correspondence of the fast polarization direction with the local geology, such as the Appalachians. More specifically they calculated a dominant NE-SW orientation of the fast polarization direction along the eastern margins of North America, however found an E-W trend in the southern margin (Barruol *et*

al.,1997). All measurements were parallel to local orogenic features that originated from past deformation events such as the Grenvillian deformation (Figure 5).

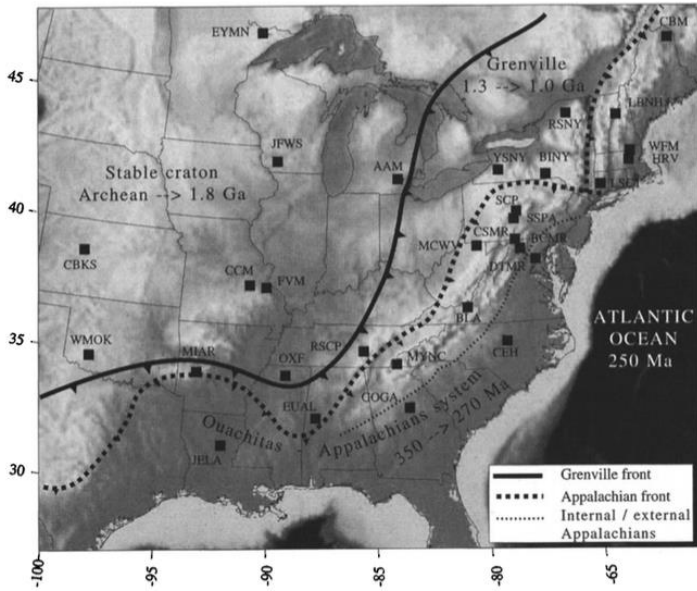


**Fig. 5:** A topographic map displaying time span of orogenic boundaries (Appalachians and Grenville) and station locations across the eastern U.S (From Barruol *et al.*, 1997).

Overall, Barruol *et al.*, (1997) establishes a correlation of shear wave splitting parameters with local surface geology. In addition, there is weak and complex anisotropy with signatures from fossil tectonic fabric and the subcrustal lithosphere. However, there remains some uncertainty with these results since the lithosphere is a complex structure with contributions from many processes. Finally, they suggest additional collection of seismic data to further examining the zones where anisotropy varies.

Similarly, Levin *et al.*, (1999) focused on shear wave splitting (SKS, SKKS, PKS) in the northern Appalachians and the Urals (Russia) and compiled data from the longest running stations at the time: HRV (Harvard, MA), PAL (Palisades, NY), and ARU (Arti, Russia). More



importantly, they collected data from a wide range of backazimuths and angles of incidence. They observe that the eastern and northeastern orientations dominate the fast polarization direction, suggesting that both mountain belts have a strong influence on complexity (Figure 6).

**Fig. 6:** A map of the northeastern Appalachians with plotted seismic anisotropy measurements (arrows) that represent the fast direction. Note how the splitting trend follows an eastern direction. (From Levin *et al.*, 1999)

Levin *et al.*, (1999) also use synthetic data to develop an anisotropic model for HRV, which

results in two anisotropy layers below an isotropic crust. In addition, they emphasize the importance of past continental collisions and accretion for anisotropy in the tectosphere (Levin *et al.*, 1999). Specifically, the local absolute plate motion, which is representative of the asthenosphere, highly influences the observed complex anisotropy. They conclude that there are multiple anisotropic layers within the mantle from shear wave splitting observations over extensive backazimuthal coverage.

Aside from shear wave splitting, there are surface wave techniques that provide insight on mantle anisotropy. Surface wave analysis further constrains anisotropy in the mantle, serving as a complement for shear wave splitting. This analysis provides detailed vertical resolution at certain depths (Long and Becker, 2010). For example, Deschamps *et al.*, (2008) analyzed anisotropy in East-central U.S., south of my region of interest. However, they also found evidence for Appalachian anisotropy in the southeastern United States. They developed a three-layered model of anisotropy using surface-wave array analysis. More, specifically, they measured Rayleigh-wave phase velocities comparing them to observed anisotropy from SKS splitting. In addition, they are able to further constrain anisotropy to three distinct layers beneath the orogen using this different technique. Like previous studies, they also observed fast wave propagation in the direction of the Grenville and Appalachian orogens, which illustrates the influence of past continental collisions on the deformation of the lower crust and upper mantle (Deschamps *et al.*, 2008). From this data they reconstruct an estimated timeline displaying past deformation events and their role in seismic anisotropy (Figure 7).

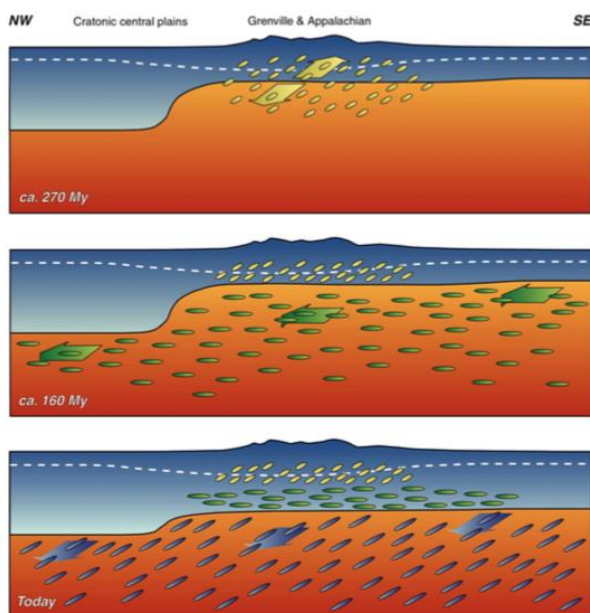


**Fig. 7:** Schematic diagram outlining progression of events that reflect current anisotropic signals after the Appalachian orogeny. First, there was extensive deformation in lower crust and upper mantle at 270 Ma, followed by a thickening of the lithosphere at 160 Ma. Both deformation events contribute to frozen seismic anisotropy near the orogen. Today North American plate motion contributes to deformation and anisotropy in the asthenosphere. (From Deschamps *et al.*, 2008)

Overall, Deschamps *et al.*, (2008) successfully constrains signals from different layers and attributes each one to a past deformation event. They determine fast polarization directions in the lithosphere parallel to the Grenville and Appalachian orogens, which are representative of a frozen fabric in the lower crust and upper mantle. However, the lower lithosphere has fast polarization directions parallel to the North American plate motion and correlates with relative age (160-125 Ma) after the orogen. Finally, current plate motion and deformation contribute to anisotropic signatures from the asthenosphere. With these constraints, Deschamps *et al.*, (2008) clearly uses anisotropic signatures to demonstrate the development of the lithosphere across past deformation events in the central and southeastern United States.

Long *et al.*, (2010) conducted shear wave splitting and receiver function analyses at seismic stations to determine mantle dynamics across the southeastern United States. More specifically receiver function analysis constrains the timing of earthquake arrivals providing information on transition zone thickness. They collected five years of data at eleven long-running stations scattered across the interior and coastal parts of the North American continent. The results cover a range of backazimuths, which further supports their model and allows for a comparison with previous predictions.

First, they observed an absence of shear wave splitting (null behavior) for stations closer to the coastal southeastern United States suggesting an isotropic upper mantle (Long *et al.*, 2010). However, stations located further inland displayed splitting behavior consistent with the NE-SW fast polarization direction. They attribute this splitting pattern to the Appalachian tectonic structure as well as the current absolute plate motion (Long *et al.*, 2010). Therefore, there is a stronger presence of shear wave splitting near the interior of the continent (Figure 8).

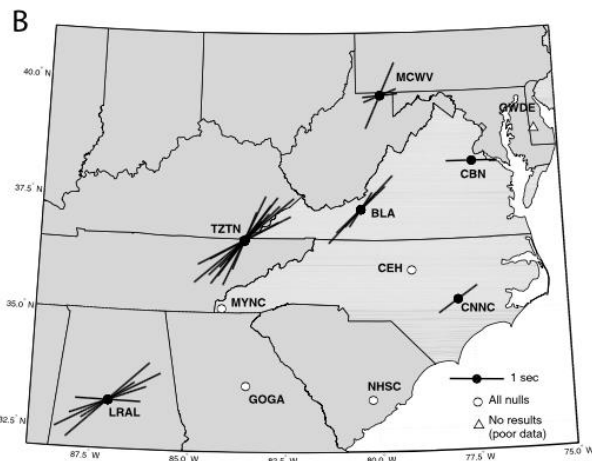


**Fig. 8:** Map of stations along the southeastern U.S. with plotted SKS splitting results represented as black bars oriented in the fast polarization direction. Null stations are represented by white circles. Note how SKS splitting dominates further inland, while null results lie closer to the coast. (From Long *et al.*, 2010)

Finally, they conclude that there is a transition from a horizontal mantle flow (absolute plate motion) to a vertical mantle flow (upwelling or downwelling) as the stations move from the Appalachians (interior) to the coast (edge). In addition, they match transitional zone thickness estimates to observed global averages, further constraining this scenario. Long *et al.*, (2010) recognize that denser seismic networks, such as the Transportable Array and Flexible Array, will yield additional data to determine detailed mantle dynamic models in the future.

Recently, Long *et al.*, (2016) performed an extensive SKS splitting analysis on the Transportable Array (TA) in eastern North America. The TA network provided data that spanned 10-12 months and covered extensive geographic area. In the northern area, they detected the presence of a complex anisotropic structure, characterized by a mix of null and SKS splitting dominated stations. Like previous studies, Long *et al.*, (2016) also observed that stations at high topographies (NE Alabama to PA) displayed a fast polarization directions parallel to this Appalachian mountain range. This implies that past Appalachian lithospheric deformation contributed to the complex anisotropy beneath the continental plate. However, in the southeastern United States (Coastal Plains), they documented predominantly null results with extensive backazimuthal coverage (Long *et al.*, 2016). Finally, in the southern area of the U.S. they yielded EW to NE-SW fast polarization directions potentially signal past deformation events. The map below displays the comprehensive patterns of SKS splitting along the eastern United States (Figure 9).

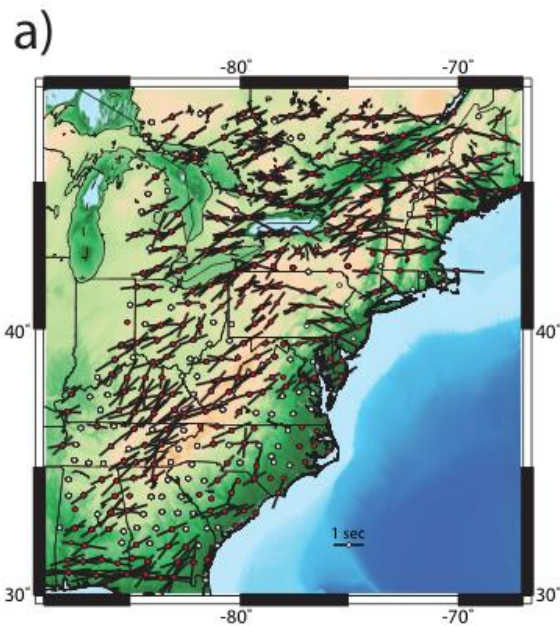


**Fig. 9:** Map of eastern Transportable array displaying stations with SKS splitting measurements (black bars) oriented with the fast direction as well as stations with primarily null measurements (white circles). See explanation for visible patterns above (From Long *et al.*, 2016)

Long *et al.*, (2016) recommend future studies that encompass SKS splitting, surface wave, and receiver function analyses will constrain the vertical and lateral variability of anisotropy, as well as, distinguish contributions from the lithosphere and asthenosphere from null results. Overall, seismic anisotropy below eastern United States continues to be complex with

contributions from various sources as shown throughout these studies. Although some of these studies focus on the southern and central areas of the eastern United States, they provide the necessary framework for understanding the influence of past deformation on seismic anisotropy. More specifically, my study builds on these previous findings by thoroughly investigating multiple layer anisotropy at long-running stations. I use the SKS wave splitting technique presented in all of these studies to constrain signals from the lithosphere and the asthenosphere as well as present and past deformation. Similarly, I also provide data with a range of backazimuthal coverage, but over a longer time period allowing for a detailed analysis on complex anisotropic layering.

#### IV. Shear Wave Splitting Methodology

Shear wave splitting reflects the seismic anisotropy along a specific ray path. At the core mantle boundary, there is polarization of SKS waves because of the transition from P to S waves, since there is a conversion of liquid/solid (core) to solid material (mantle). This quantitative approach provides detailed lateral resolution since the SKS wave follows a vertical ray path, however, depth resolution is limited (Long and Silver, 2009). After an earthquake, an SKS wave will travel through the mantle, pass briefly through the outer core, and enter the mantle again until it reaches the seismic station at the surface (Figure 10).

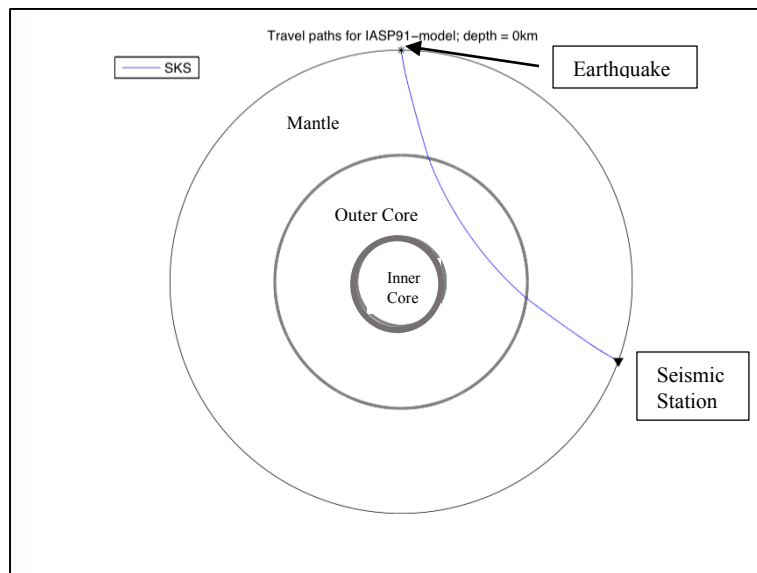


**Fig. 10:** Ray-path of SKS phase used for this study shown as a solid blue line, which starts from the earthquake travels through Earth's interior until it is picked up by seismometer. (Generated using SplitLab software)

In addition, a travel time curve displays the estimated arrival times where one should expect an SKS wave. When analyzing seismograms the selected earthquake window must correlate with the theoretical arrival time of an SKS

wave before proceeding with splitting measurements. The following figure illustrates travel times for various P and S waves, including SKS (Figure 11).

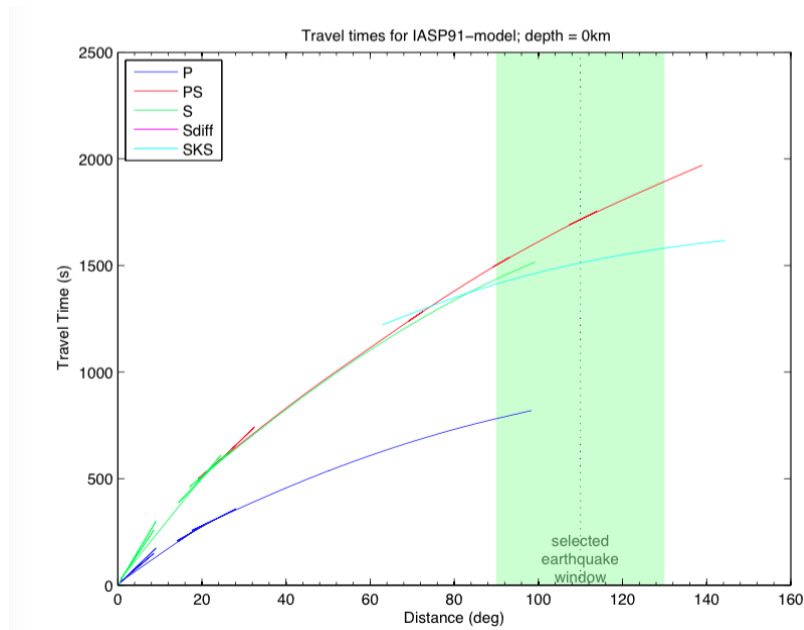


**Fig. 11:** Travel time graph showing distance traveled over time for various types of waves including SKS (light blue). SKS arrival corresponds to predicted calculations. Green box indicates selected earthquake window. (Generated using SplitLab software)

More specifically, I defined my events as earthquakes with a magnitude greater than 5.7 M and selected an earthquake window between 90° and 130° as shown above. Once I configured my project, the SplitLab software in MATLAB produced earthquake seismograms for each event in my list (Wüstefeld *et al.*, 2008). The statistic plot below represents data from station HNH in New Hampshire, displaying the number of earthquake events relative to their backazimuthal estimations (Figure 12).

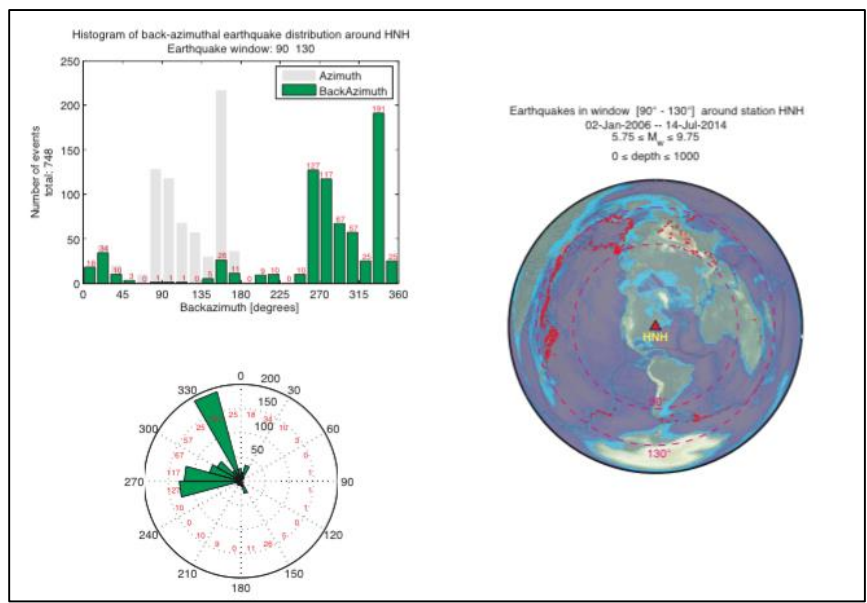


**Fig. 12:** Three methods of conveying backazimuthal coverage for HNH from 2006-2015. Top left histogram displays the backazimuthal distribution of events, while bottom left also illustrates this in a rose plot. Finally, on the right, there is an azimuthal map that shows event locations around the world relative to the station. Note backazimuths ~270° and ~330° dominate earthquake events (Generated using SplitLab software)

On a three-component seismogram, the faster polarized shear wave will arrive first on the north-south axis, followed by the slower polarized shear wave on the east-west axis. More specifically, after an earthquake, P, S, and surface waves will behave differently on seismograms. For example, an S wave has transverse motion that is visible on the East-West component of the seismogram and will arrive later. However, a compressional P wave will exhibit motion earlier on the vertical component, since it has longitudinal propagation and arrives first travelling twice as fast as an S wave. Finally, surface waves follow immediately after and affect all three components. Therefore, each wave has its respective component, so one can successfully pinpoint the arrival of an SKS wave for splitting measurements and analysis.

While reviewing events from SplitLab, I applied a bandpass filter of 0.01-0.1 Hz to each seismogram to remove noise and enhance SKS arrivals. Depending on the quality of SKS arrival, I also applied another filter of 0.04-0.125 Hz to each individual event. The following seismogram displays the clear arrival of an SKS wave at the expected time with a bandpass filter of 0.04-0.125 Hz. Once I identified an SKS arrival, I selected an earthquake window for splitting parameters and future interpretation (Figure 13).

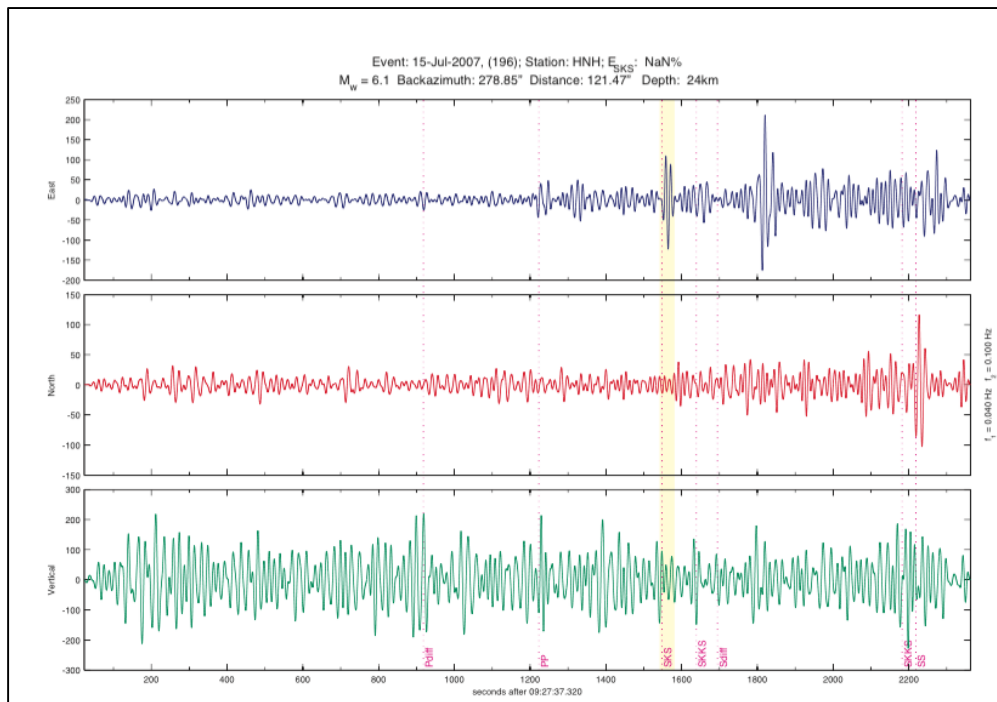


**Fig. 13:** Seismogram from HNH station in New Hampshire divided into three components each expressing various arrivals of waves, such as SKS. Highlighted is the selected earthquake window for SKS splitting parameters and future analysis. (Generated using SplitLab software)

Next, SplitLab produced particle motion diagrams for each SKS arrival, which I analyzed to determine whether splitting has occurred (Wüstefeld *et al.*, 2008). More specifically, the particle motion, linear or elliptical, must be in the same direction as the backazimuth. For example, a null measurement indicates that there is no splitting at the arrival of an SKS wave, which may suggest apparent isotropy in the medium. Null results are characterized by linear particle motion that vibrates parallel to the backazimuth. In this study, nulls were categorized into 3 types: good, fair, and poor quality. The criteria I used to evaluate each measurement included: the initial quality signal, the ellipticity of particle motion, the corrected linear particle motion, and the coherence between fast and slow split shear waves (Barruol *et al.*, 1997). Once I confirmed the particle motion, the SplitLab software created a diagnostic plot of my null measurements. SplitLab uses three techniques to remove the effect of splitting linearizing particle motion in its calculations: rotation-correlation, minimum energy, and eigenvalue method (Wüstefeld *et al.*, 2008). The transverse component minimization method used by SplitLab reduces the transverse component's energy and creates a corrected linear particle motion in the absence of anisotropy (Long and Silver, 2009). Overall, the SplitLab software was used to calculate shear wave splitting measurements from best-fit splitting parameters: the fast polarization direction ( $\varphi$ ) and time delay ( $\delta t$ ). The following diagram illustrates a good null retrieved from station HNH in New Hampshire, with linear particle motion polarized nearly parallel to a backazimuth of  $333.4^\circ$  a fast polarized direction of  $-29^\circ$ , and delay time of 2.5s (Figure 14, see caption on following page).

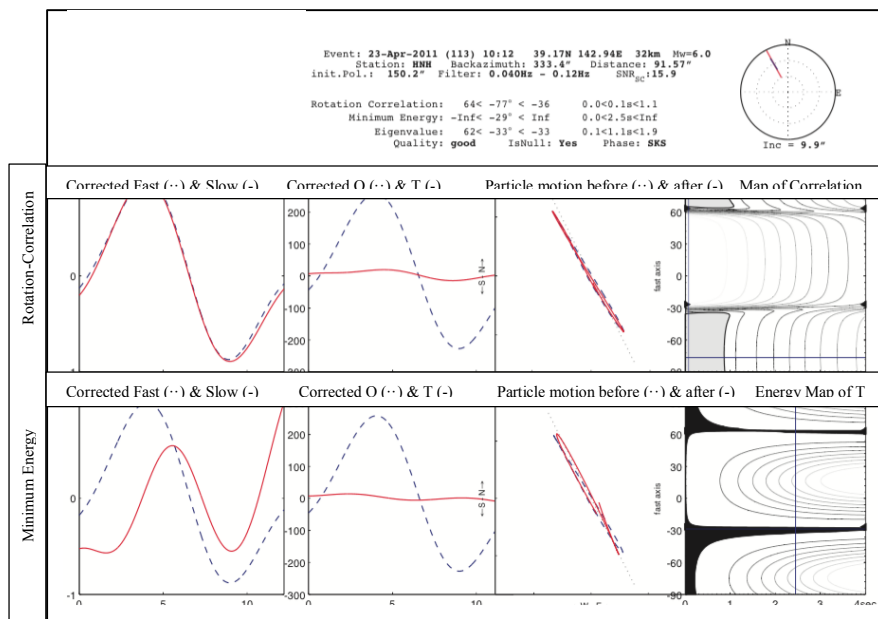


**Fig. 14 (Above):** This diagnostic plot displays a null measurement from station HNH. First panel displays calculations from the rotation-correlation method. Second panel contains results using the transverse component energy minimization method. There is no apparent evidence of splitting due to the fast direction of the particle motion vibrating in same direction of backazimuth. (Generated using SplitLab software).

An elliptical particle motion characterizes a split measurement that occurs in an anisotropic medium (Long and Silver, 2009). As seen above, SplitLab also produces a contour plot with an energy map of the transverse component and a map of the correlation coefficient. If there is shear wave splitting, the two measurement methods, rotation correlation and minimum energy values, must agree and cannot differ by more than  $\sim 20^\circ$ . In addition, when looking at the maps of both parameters, the error spaces must be superimposed and well constrained in a small area. The error space should be an ellipse that constrains the data. The diagram in Figure 1 from Long and Silver, (2009) displays an example of a high-quality splitting measurement with high delay time calculated from best-fit splitting parameters (Figure 15). The long axis of the ellipse follows the direction of the backazimuth and both the rotation correlation and minimum energy have very similar values. In addition, the data is very well constrained as seen through the grey shaded area; therefore it can be said with confidence that there is SKS splitting at this particular event.

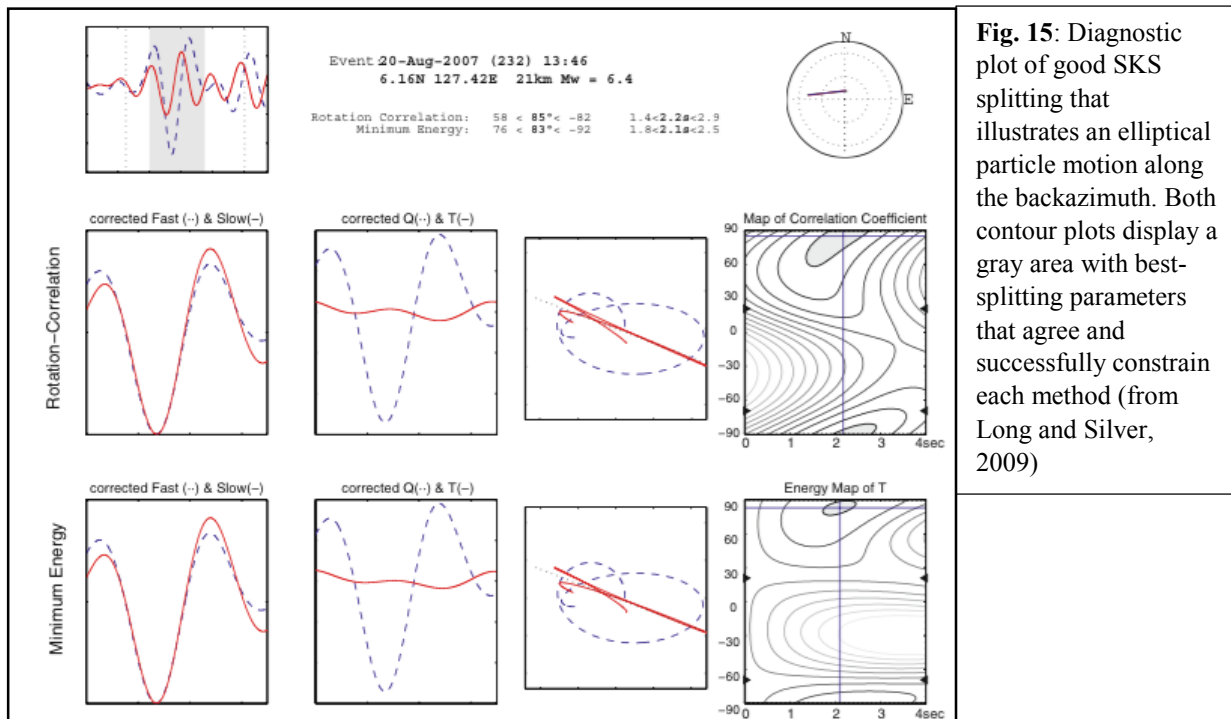


**Fig. 15:** Diagnostic plot of good SKS splitting that illustrates an elliptical particle motion along the backazimuth. Both contour plots display a gray area with best-splitting parameters that agree and successfully constrain each method (from Long and Silver, 2009)

The time delay between arrivals of slow and fast shear wave provides information on the density of cracks in the anisotropic medium. Some factors that affect the delay time include the degree (strength) of anisotropy and the length of distance a wave travel through Earth’s interior to the seismic station (Levin *et al.*, 1999). Finally, the fast polarization direction of an SKS represents the structure and geometry of anisotropy (Long and Silver, 2009). Sometimes past and present deformations cause the fast polarization direction to have a certain orientation. When analyzing SKS results, a wide range of backazimuths constrains signals in the upper mantle, whether it be from the asthenosphere or lithosphere, and determines the amount of anisotropic layers below the crust. Overall, the SplitLab software allows for users to design and execute SKS splitting analyses from large datasets (Wüstefeld *et al.*, 2008). More specifically, it uses various techniques to produce the best-fit parameters and constrain results in contour plots. It is both an efficient and interactive program that expedites data processing in seismological research.

**V. Data and Results**

For this study, I looked at seven long-running seismic stations across the Northeastern United States. These seismic stations listed below provided extensive geographic and temporal coverage (Table 1). For all the stations, I requested data from the IRIS Data Management Center, however there were gaps of missing events in the time range as noted in Table 1. Despite receiving less data than anticipated, there were still around 500 events per seismic station with extensive backazimuthal coverage and provided evidence for both null and split measurements.

Network	Station Code	Lat, Long.	Time Range
NE	HNH	43.71, -72.29	2006-2014
NE	TRY	42.73, -73.67	1995-2013*
NE	QUA2	42.28, -72.35	1995-2016
NE	PQI	46.67, -68.02	1999-2016
LD	UCCT	41.79, -72.22	2005-2014*
IU	SSPA	40.64, -77.89	1994-2014
US	BINY	42.19, -75.98	1993-2016

**Table 1:** The above table displays network, station code, location coordinates, and time period for which data was recorded and analyzed for shear wave splitting. \*Indicates gaps where there were missing events in observed time ranges.

As previously mentioned, I performed shear wave splitting analyses and produced diagnostic plots for these stations using the SplitLab software in MATLAB. I also created

stereoplots to help visualize the distribution of splitting and null results based on the backazimuth, incidence angle, fast direction, and delay time. For station HNH, I collected about fifty null measurements and categorized the majority as good null measurements. A backazimuth range from around  $\sim 270^\circ$  to  $\sim 330^\circ$  dominated the null measurements, but overall this station provides good backazimuthal coverage. Stereoplot HNH illustrates the concentration of null measurements along backazimuthal values between  $\sim 270$ - $330^\circ$  based on fast polarization directions (Figure 16a). For station UCCT I identified only null arrivals, with limited backazimuthal coverage due to limitations with data retrieval. Each of the six null measurements corresponds to a distinct backazimuth based on the delay time and fast direction parameters. Stereoplot UCCT displays the sparse data null data from SKS arrivals (Figure 16b). Finally, I documented one null measurement for station TRY due to difficulties in requesting seismic events from the data center and included it below for completeness (Figure 16c).

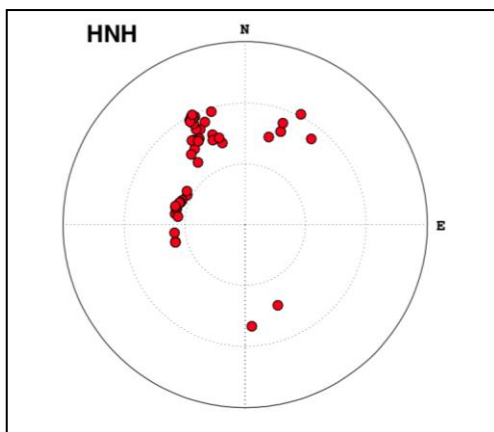


**Fig. 16a:** Stereoplot for station HNH displaying null results represented by red circles. This station had good backazimuthal coverage.

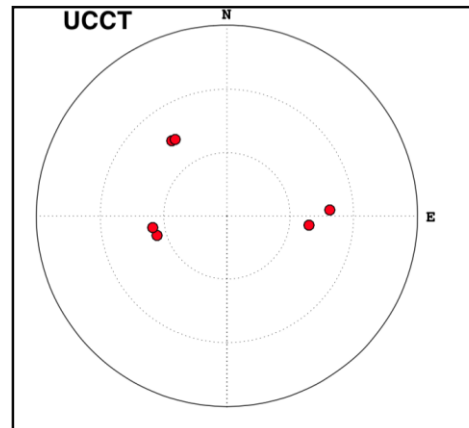


**Fig. 16b:** Stereoplot for station UCCT displaying six null results represented by red circles. There was limited backazimuthal coverage

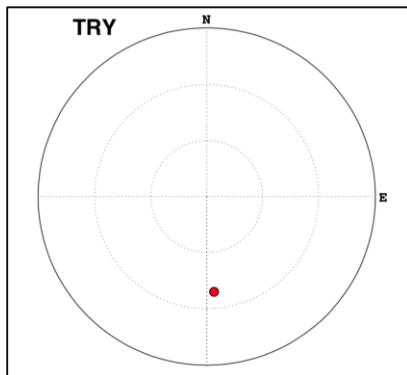


**Fig. 16c:** Stereoplot for TRY with single null result. Significantly less data due to unforeseen problems with seismometer.

For station QUA2, I sampled seventeen earthquake events and obtained fair to weak splitting measurements for two events. The fast polarization directions for the SKS splitting measurements overlap with the general backazimuthal trend covered by the nulls (Figure 17a). Similarly, PQI also displayed weak splitting at two out of eight total events, the rest were nulls (Figure 17b). At station SSPA, I collected thirty-five null measurements and one split measurement with acceptable backazimuthal coverage (Figure 17c). The fast polarized fast directions of the null results tend to be concentrated around backazimuths ranging from  $\sim 250^\circ$  to  $\sim 330^\circ$ . The single split result has a backazimuth of  $25^\circ$ , a fast polarized direction of  $75^\circ$ , and delay time of 0.7 seconds. Finally, station BINY provided a total of twenty-five measurements, with four weak splitting results over good backazimuthal coverage (Figure 17d). Two of these split measurements fell within the backazimuthal range of approximately  $\sim 310^\circ$ - $330^\circ$  consistent with previous results.

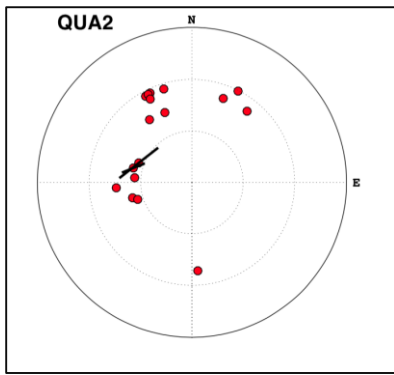


**Fig. 17a:** Stereoplot QUA2 shows null measurements (red circles) over some backazimuthal coverage (N-W), with few splitting measurements represented by black bars oriented in the fast polarized direction.

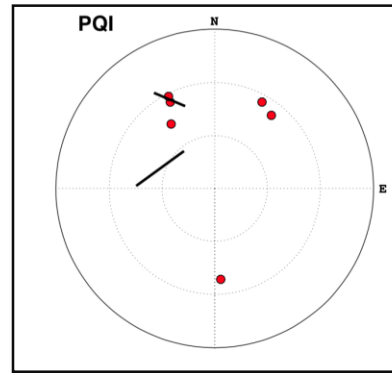


**Fig. 17b:** Stereoplot PQI displays fewer null measurements with poor backazimuthal coverage. There are two weak splitting measurements with distinct fast polarized directions.

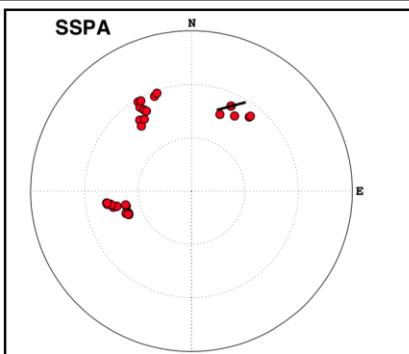


**Fig. 17c:** Stereoplot SSPA shows majority of null measurements with one split measurement located among a cluster of nulls in the NE orientation.

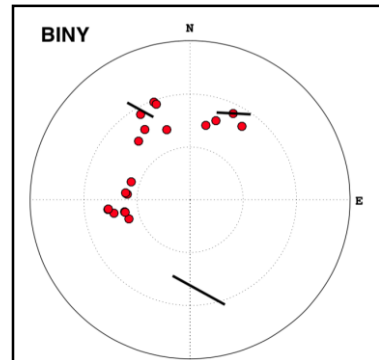


**Fig. 17d:** Stereoplot BINY displays nulls with extensive backazimuthal coverage as well as several split measurements that fall within that range.

However, for the majority of SKS splitting measurements across all stations it was difficult to constrain the rotation correlation and minimum energy values, so most measurements were categorized as fair. The diagnostic below displays best-fit splitting parameters for a fair QUA2 event with a backazimuth of  $283.7^\circ$ , fast direction of  $68^\circ$ , and delay time of 0.6s (Figure 18). The nearly elliptical motion along the backazimuth is indicative of weak splitting, but we must consider particle noise as well as other possible disturbances. This result is representative of all splitting measurements, in terms of weak constrains and elliptical particle motion.

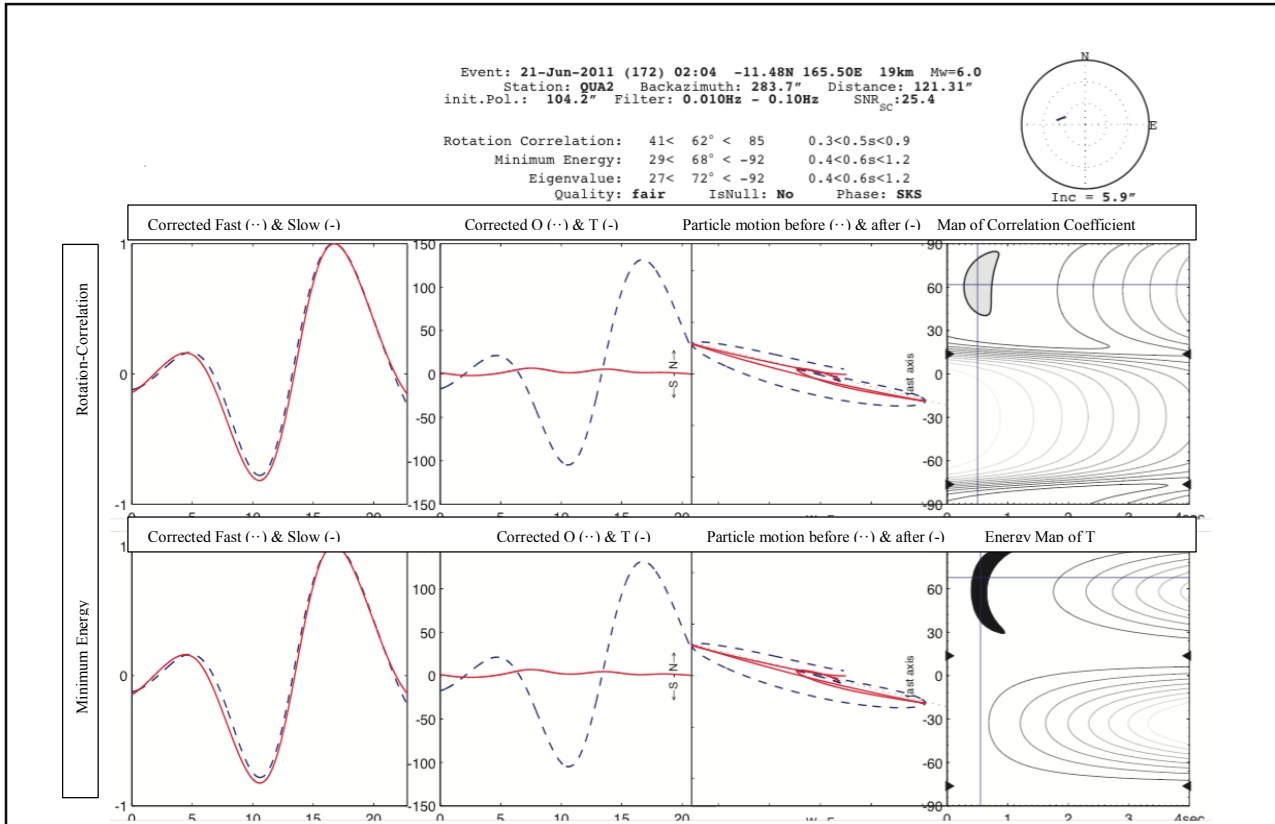


**Fig. 18:** QUA2 diagnostic plot for weak splitting measurement that illustrates what characterizes the fair category of SKS splitting. For example, there is significant particle noise, in addition to being loosely constrained in the grey areas (Generated using SplitLab software).

## VI. Discussion and Implications

The results of this study contribute to previous work along the eastern United States. For example, station HNH is a null station with null splitting with the best backazimuthal coverage. SKS splitting is absent from this location. Therefore, there is apparent isotropy at this station, which may be the result of multiple layers cancelling out the anisotropic signal. More specifically, a shallow, upper layer beneath HNH obscures any underlying anisotropy. Therefore, there is the

possibility of weak anisotropy at this station. Previous studies have also identified anomalous areas where null behavior dominates certain stations. More specifically, Barruol *et al.*, (1997) first suggested that several splitting stations surrounded station CEH in North Carolina, which exhibited only null behavior. In addition, Long *et al.*, (2010) further confirmed these results, when they collected a large number of nulls at this station with extensive backazimuthal coverage. Although, station HNH is in the northeast, while CEH is in the southeast coast of the United States, they both express similar patterns in a much broader context. Long *et al.*, (2010) presents four mantle flow scenarios to interpret their results. I believe this isolated region of null measurements at HNH most likely aligns with the third mantle flow model of multiple layers of anisotropy. This occurs when two layers of anisotropy produce equal time delays that are offset by  $\sim 90^\circ$  cancelling each other out and eliminating the anisotropic signature (Long *et al.*, 2010). Station HNH measurements reflect complex anisotropy at this locality that must be further studied and constrained to fully understand the mechanism that induces null behavior.

Similarly, station UCCT also displays null behavior, but with limited backazimuthal coverage. At this station, there were significantly less results due to data retrieval issues. More specifically, the data center only provided a fragment of the recorded events, despite the long-running time. However, this null behavior is also consistent with multiple layers of anisotropy, which suggests that variations may occur on the small scale in the lithosphere. This local behavior cancels out possible anisotropy signals coming from deeper within the mantle. Finally, at station TRY there were only one hundred events available for analysis. From these one hundred events, I identified one null measurement and included that information to represent the entirety of this project. Although TRY did not have enough data to make valid conclusions, I believe station TRY provides a preliminary result that reflects a hint of complex anisotropy, but further analysis is necessary to support this hypothesis. Overall, two stations display only null results with backazimuthal variation, which indicate the possibility of complex anisotropy beneath the local area.

There were also some stations that demonstrated weak splitting behavior with good backazimuthal coverage. For example, station QUA2 produced two split results among a mixture of nulls with varying fast directions that were polarized in the same direction as the backazimuth. A backazimuth value of  $\sim 250^\circ$ - $330^\circ$  (N-W) dominated the null fast polarized direction distribution. Therefore, QUA contains two splitting measurements with a N-W orientation, which in turn

suggests multiple layers of anisotropy, although both split measurements are from the same backazimuth. In addition, station PQI exhibits weak splitting from different backazimuths ( $290^\circ$  and  $333^\circ$ ) and fast directions ( $54^\circ$  and  $-67^\circ$  respectively), however these results are more variable. The backazimuthal coverage is significantly less, so it becomes difficult to assign a general orientation to the measurements. This station in particular had a significant level of noise in the seismograms, so it remains unclear whether these split results imply complex anisotropy. Nevertheless, we cannot overlook the consistent signature of multiple layers of anisotropy.

The final two stations in my study, BINY and SSPA, were also previously example by Barruol *et al.*, (1997). At the time, Barruol *et al.*, (1997) collected eight measurements at BINY and 1 measurement at SSPA. More specifically, at station BINY they determined null and non-null (split) results with E-W orientation of  $N101^\circ$  for mean fast polarization directions (Barruol *et al.*, 1997). In addition, the null SKS arrivals generally arrived at a backazimuth of approximately  $340^\circ$ , which provides good backazimuthal coverage. Barruol *et al.*, (1997) concluded anisotropy at this station is not well constrained, since there are a whole possible range of backazimuths. He attributes the strong signal of the  $\sim 340^\circ$  backazimuth to the large number of events that originate from subduction zones in the western Pacific. This accounts for the backazimuthal range of  $\sim 300^\circ$ - $340^\circ$  of these results, as well the results I present here. Finally, Barruol *et al.*, (1997) also confirms that his BINY measurements are consistent with a previous study performed by Levin *et al.*, (1996). Unfortunately, the single measurement at SSPA, similar to my TRY result, cannot be extrapolated to reflect complex anisotropy in the northeastern United States.

Today, station BINY provides over 20 years of seismic data and possibly additional information that confirms the results of Barruol *et al.*, (1997). Specifically, BINY produced twenty-two null measurements and three split measurements with fairly consistent fast polarization directions. The presence several split measurements indicates the possibility of weak splitting and complex anisotropy over a wide range of backazimuths. Like Barruol *et al.*, (1997), my two split measurements follow a backazimuthal trend from  $\sim 300^\circ$ - $340^\circ$ , specifically backazimuthal values of  $331^\circ$  and  $312^\circ$ , with fast polarization directions of  $-61^\circ$  and  $6^\circ$  respectively. There is also another null with a backazimuth of  $27^\circ$  and fast polarization direction of  $-87^\circ$ . Overall, the backazimuthal distribution of null measurements and weak presence of splitting suggest the presence of multiple layers of anisotropy, although additional data could further characterize this.

Finally, station SSPA also exhibited signals of weak splitting. More specifically, one split measurement with backazimuth of  $25^\circ$  and fast polarization direction of  $75^\circ$  among nulls clustered in specific backazimuths such as  $\sim 25^\circ$ ,  $\sim 250^\circ$ , and  $\sim 330^\circ$ . Unfortunately, the scattered backazimuths do not provide the necessary constraints for further complex anisotropy observations. Like Barruol *et al.*, (1997) measurements at SSPA remain ambiguous compared to other stations that have a more consistent range of backazimuths.

Overall, HNH and UCCT exhibited only null behavior, while the rest of the stations display evidence of weak splitting. The large amount of null measurements at HNH indicates apparent local isotropy, where one or two layers may block anisotropic signals from deeper within the mantle. Stations surrounding UCCT and HNH display minimal SKS splitting measurements with good backazimuthal coverage. Backazimuthal variations constrain the presence of multiple layers in the lithosphere and asthenosphere, however we cannot rule out other scenarios that explain complex anisotropy. In addition, the majority of station measurements are consistent with multiple layers of anisotropy as previously recorded in earlier studies such as Barruol *et al.*, (1997), Levin *et al.*, (1999), and Long *et al.*, (2010). Today, absolute plate motion as well as past deformation contribute to the wide distribution of null and split measurements recorded at these stations. From these stations, complex anisotropy from weak splitting characterizes the northeastern United States.

## **VII. Limitations and future work**

One of the most common problems in seismic anisotropy studies is the limited amount of events. Despite requesting data from long-running stations, not all the events were available for analysis. In addition, some of the seismometers were misoriented and captured high levels of noise. It is also important to have data with extensive backazimuthal coverage, which unfortunately some stations did not have. This possibly impacted some of the measurements at several stations creating uncertainty with some of the interpretations. In addition to data retrieval issues, the SKS splitting technique itself also has some limitations. For example, Long *et al.*, (2016) acknowledge that SKS splitting measurements in continental settings have poor depth resolution. More specifically, SKS follow a vertical ray path as they travel in the upper mantle, which limits depth resolution, but provides detailed lateral resolution (Long *et al.*, 2016). Also, the SKS splitting technique infers a single layer of anisotropy with horizontal symmetry, which may not be consistent with observed signals (Long and Silver, 2009). Barruol *et al.*, (1997) also recognizes the limitations in the

splitting parameters, fast polarization direction and delay time, since they are heavily dependent on the thickness and composition of the anisotropic layer, which further limit depth resolution. Finally, a complex tectonic and geologic setting also leads to uncertainties when analyzing anisotropic signals. Current and past deformation events lead to complex anisotropy, which at times is poorly constrained.

Therefore SKS splitting must be complemented by other techniques such as surface wave analysis and receiver function analysis to overcome some of its shortcomings and further constrain results. For example, surface waves provide additional constraints to seismic anisotropy analyses, since they propagate horizontally across the upper mantle and crust. More specifically, at depths that are one third of the wavelength, surface waves reflect structural changes and transitions in Earth's interior (Deschamps 2008) Therefore, they provide high vertical resolution only in this depth range, while SKS splitting provides the necessary lateral resolution. Finally, receiver function analysis further constrains anisotropy in the crust by providing vertical resolution from Ps seismic phase conversions at the mantle to core transition (Long *et al.*, 2010) In addition, receiver function analysis also reflects the geometry and structure of the interior providing insight on dynamic processes as well. (Long *et al.*, 2010).

A comprehensive surface geology analysis also provides constraints on the variations in the fast polarization direction and delay time. Barruol *et al.*, (1997) emphasizes the controversy on whether past tectonic events or various present day processes contribute to the asthenospheric flow beneath an isotropic plate. This further complicates the interpretation of intrinsic anisotropy. In addition, the lithosphere is subject to many perturbations, which contributes to the ambiguous anisotropy. However, Barruol *et al.*, (1997) documents a strong correlation between SKS splitting parameters and surface geology and attributes complex anisotropy to fossil tectonic fabrics and the subcrustal lithosphere. Therefore, geologic trends (N-S) along the northeastern U.S. may provide further insight on complex anisotropy and why certain areas exhibit only null measurements, while others show a mixture of null and split measurements.

As we move forward with this data, the next step is to develop detailed forward modeling that distinguishes between the contributions from the lithosphere and asthenosphere to seismic anisotropy. Silver and Savage (1994) present a forward model on the San Andreas Fault system providing a theoretical framework, from derived expressions and trigonometric functions, to model multiple layers of anisotropy. They interpret their results and conclude that their model is

consistent with the presence of two anisotropic layers, which can be applied to similar scenarios such as the work presented here.

### **VIII. Summary and conclusion**

Overall, in this study, I conducted SKS splitting measurements at seven long-running stations across the northeastern United States. In general, the data is consistent with multiple layers of anisotropy, although there is not enough data to further characterize this. Backazimuthal variations in the data suggest the presence of one layer of anisotropy in the asthenosphere and a shallower layer in the lithosphere. However, there remain uncertainties and other scenarios such as an isotropic layer cannot be ruled out. In addition, limited depth resolution further obscures contributions from the lithosphere and asthenosphere. Two stations, HNH and UCCT, contained only null results, while surrounding stations exhibited fair shear wave splitting. This project serves as a continuation for previous seismic anisotropy work in the eastern United States as we continue to demystify past deformational processes and their role in shear wave splitting signatures. Additional work is required to constrain our interpretations of multiple layer anisotropy in the context of present day mantle flow and other subsurface processes.

### **Acknowledgements**

I wish to express my sincere gratitude to my adviser, Maureen Long, for constantly supporting me throughout this project. When I approached her last semester about working on one her current projects, she was more than happy to mentor and guide me through the process. This study could not have been possible without her. Thank you for your patience and kindness, it was truly a joy to work with someone who is very passionate and excited about seismological research! The seismic data used for this study was acquired from the IRIS Data Management Center and processed using the efficient SplitLab software in MATLAB. Finally, I would like to thank Dave Evans for encouraging me to pursue geology and geophysics and being a constant source of motivation. Thank you to the Geology and Geophysics department, which has been a welcoming community for the last four years.

## References

- Barruol, G., Silver, P.G., and A. Vauchez (1997). Seismic anisotropy in the eastern United States: Deep structure of a complex continental plate. *Journal of Geophysical Research* **102** (B4): 8329-8348
- Deschamps, F., Lebedev, S., Meier, T. and J. Trampert (2008). Stratified seismic anisotropy reveals past and present deformation beneath the East-central United States. *Earth and Planetary Science Letters* **274**: 489-498
- Hatcher, R. D. (2010). The Appalachian orogeny: A brief summary, in *From Rodinia to Pangea: The Lithotectonic Record of the Appalachian Region*, edited by R.P Tollo *et al.*, 1-19 Geological Soc. Of Am., Boulder, Colo
- Levin, V., Menke, W., and J. Park (1999). Shear wave splitting in the Appalachians and the Urals: A case for multilayered anisotropy. *Journal of Geophysical Research* **104** (B8): 17975-17993
- Long, M. D. and T. W. Becker (2010). Mantle Dynamics and Seismic Anisotropy. *Earth and Planetary Science Letters* **297**: 341-354
- Long, M.D., Benoit, M. H., Chapman M. C., and S. D. King (2010). Upper mantle anisotropy and transition zone thickness beneath southeastern North America and implications for mantle dynamics. *Geochemistry, Geophysics, Geosystems* **11** (10): 1-22
- Long M. D., Jackson, K. G., and J. F. McNamara (2016). SKS splitting beneath Transportable Array Stations in eastern North America and the signature of past lithospheric deformation. *Geochemistry, Geophysics, Geosystems* **17**: 2-15
- Long, M. D. and P.G. Silver (2009). Shear wave splitting and mantle anisotropy: Measurements, interpretations and new directions. *Survey of Geophysics* **30**: 407-461
- Silver, P. G. and M. K. Savage (1994). The interpretation of shear-wave splitting parameters in the presence of two anisotropic layers. *Geophysical Journal International* **119**: 949-963
- Stoffer, P. and P. Messina. Origin of the Appalachian Orogen, Available from: [3dparks.wr.usgs.gov/nyc/images/fig53.jpg](http://3dparks.wr.usgs.gov/nyc/images/fig53.jpg) (Accessed 30 April 2016)
- Wagner, L. S., Long, M. D., Johnston, M. D., and M. H. Benoit (2012). Lithospheric and athenospheric contributions to shear-wave splitting observations in the southeastern United States. *Earth and Planetary Science Letters* **341-342**: 128-138
- Wüstefeld, A., Bokelmann, G., Zaroli, C., and G. Barruol (2008). SplitLab: A shear-wave splitting environment in MatLab *Computers & Geosciences* **34**: 515-528